Journal of Alloys and Compounds 505 (2010) 367–373

Contents lists available at ScienceDirect

Journal of Alloys and Compounds

journal homepage: www.elsevier.com/locate/jallcom

A mechanism study of synthesis of $Li_4Ti_5O_{12}$ from TiO_2 anatase

Tao Yuan, Rui Cai, Ran Ran, Yingke Zhou, Zongping Shao*

State Key Laboratory of Materials-Oriented Chemical Engineering, College of Chemistry & Chemical Engineering, Nanjing University of Technology, No. 5 Xin Mofan Road, Nanjing 210009, PR China

ARTICLE INFO

Article history:
Received 4 March 2010
Received in revised form 19 April 2010
Accepted 24 April 2010
Available online 18 June 2010

Keywords:
Lithium titanate
Combustion synthesis
Solid-state reaction
Titanium dioxide

ABSTRACT

The formation mechanism of a spinel-type lithium titanate $Li_4Ti_5O_{12}$ with TiO_2 anatase as raw material, in both a conventional solid-state reaction (SSR) and a cellulose-assisted glycine-nitrate combustion (cellulose-GN) process are comparatively studied. XRD characterization demonstrates high-purity $Li_4Ti_5O_{12}$ forms at 750 °C by the cellulose-GN synthesis, which occurs at a temperature at least 100 °C lower than that via SSR. The solid-phase reaction between TiO_2 and lithium compounds to form Li–Ti–O spinel and the phase transition of TiO_2 from anatase to "inert" rutile phase occur competitively during both synthesis processes. SEM results suggest that the solid precursor from the cellulose-GN process has a smaller particle size and a more homogenous mixing of the reactants than that in the SSR. Temperature-programmed oxidation experiments demonstrate that cellulose thermal pyrolysis creates a reducing atmosphere, which may facilitate the oxygen-ion diffusion. Both factors facilitate the formation of Li–Ti–O spinel, while the TiO_2 anatase transforms to TiO_2 rutile during the SSR, which has slow lithium-insertion kinetics. As a result, a high calcination temperature is necessary to obtain a phase-pure $Li_4Ti_5O_{12}$. Charge–discharge and EIS tests demonstrate the $Li_4Ti_5O_{12}$ obtained by the cellulose-GN process shows much better low-temperature electrochemical performance than that obtained by standard SSR. This improvement attributes to the reduced particle size due to the lower synthesis temperature.

1. Introduction

Currently, Li–Ti–O composite oxides have received much attention because of their versatile phase compositions and numerous potential applications [1–3]. The phase diagram of the Li–Ti–O system has been systematically studied by several authors [4–6]. Depending on the molar ratio of lithium to titanium, there are generally four compounds with defined phase structures seen in the Li–Ti–O system, i.e., Li_4TiO_4, (α, β, γ)-phase Li_2TiO_3, spinel ($Li_4Ti_5O_{12}$), and ramsdellite ($Li_2Ti_3O_7$) [7–9]. Among these, $Li_4Ti_5O_{12}$ has received particular interest recently because of its potential application as the anode material in lithium-ion (Li-ion) batteries.

Li-ion batteries have many advantages over other types of rechargeable batteries, such as high power and energy densities, high voltage, no memory effect, no toxic battery materials, and a low self-discharge rate. As an energy-storage device, the charge/discharge processes involve lithium intercalation into and de-intercalation from the electrodes, such that the performance of Li-ion batteries depends strongly on the electrode properties. Traditional Li-ion batteries are composed of a $LiCoO_2$ layered cathode and a carbon-based anode [10,11]. These batteries have found great success in applications in the portable electronics sector. Due to environmental protection and energy-saving concerns, there is now an increasing interest in Li-ion batteries for larger-scale applications; for example, as power sources for hybrid, plug-in hybrid, and electric vehicles [12]. In these applications, high charge/discharge rates, long cycling life, and high safety are the basic requirements. However, the state-of-the-art Li-ion batteries suffer from a lack of an end-of-charge indicator in their voltage profile. There are also safety concerns because the low lithium intercalation voltage of ~100 mV at the carbon anode promotes the formation of metallic lithium, which can react with the electrolyte or the highly charged cathode, causing combustion of the organic electrolyte [13].

$Li_4Ti_5O_{12}$ is regarded as an ideal anode material for Li-ion batteries with long cycling stability due to the small lattice parameter variation during the charge and discharge processes [14]. It has a theoretical capacity of 175 mAh g^{-1} and a discharge platform of about 1.55 V versus Li/Li^+ [15], above the reduction potential of most electrolyte solvents. Therefore, highly resistant passive films from the reduction of electrolyte on the electrode surface would be less likely to form. For the same reason, the formation of metallic lithium during the discharge process can also be avoided. It is generally believed that $Li_4Ti_5O_{12}$ is a safe anode suitable for high-rate applications.

* Corresponding author. Tel.: +86 25 83172256; fax: +86 25 83172256.
E-mail address: shaozp@njut.edu.cn (Z. Shao).

0925-8388/$ – see front matter © 2010 Elsevier B.V. All rights reserved.
doi:10.1016/j.jallcom.2010.04.253

One drawback of $Li_4Ti_5O_{12}$ may be its poor electrical conductivity [16]. As a result, anodes made from coarse $Li_4Ti_5O_{12}$ show large electrode-polarization resistance at high charge/discharge rates. To circumvent this problem, surface coating with conductive film [17], doping with multivalent cations to increase the intrinsic electronic conductivity of the oxide [17], and decreasing the grain size via advanced synthesis techniques to reduce the diffusion distance and increase the interfacial surface area [18] have been tried. Traditionally, $Li_4Ti_5O_{12}$ has been synthesized by a solid-state reaction at elevated temperatures, i.e., 900–950 °C [19,20]. Such high calcination temperatures not only coarsened the powders but also increased the lithium evaporation rate, such that a poor rate performance was frequently observed.

Recently, we demonstrated that high rate-performance $Li_4Ti_5O_{12}$ electrode material can be facilely prepared by a cellulose-assisted combustion synthesis using TiO_2 anatase as the titanium source [21]. As compared with the solid-state reaction employing the same TiO_2 anatase raw material, the firing temperature for a phase-pure $Li_4Ti_5O_{12}$ was at least 100 °C lower, while the synthesis time was several times shorter. The reduced synthesis temperature and decreased calcination time then allowed the synthesis of $Li_4Ti_5O_{12}$ powders with much less aggregation and a consequently much higher electrode performance.

Understanding the mechanism of these reactions would be helpful for further optimizing the synthesis process. It may also provide guidance in the synthesis of other functional materials. In this work, a mechanistic study of the synthesis of $Li_4Ti_5O_{12}$ via the cellulose-assisted combustion technique was systematically performed. The low-temperature electrochemical performances of $Li_4Ti_5O_{12}$ produced by the combustion synthesis and by a conventional solid-phase reaction were compared.

2. Experimental

2.1. Materials synthesis and electrode fabrication

$Li_4Ti_5O_{12}$ oxide was prepared with TiO_2 anatase as the starting material by both the solid-state reaction and the cellulose-assisted glycine-nitrate combustion process. The ratio between cellulose to TiO_2 precursor is ~8 g:5 g. For details of the synthesis process, we refer the reader to our previous publication [21].

The electrochemical cycling performance of $Li_4Ti_5O_{12}$ powders was carried out with coin-shaped cells using a metallic lithium film as both the counter and reference electrodes. The cells had a configuration of Li metal (−)|electrolyte| $Li_4Ti_5O_{12}$ (+), with a liquid electrolyte (1 M solution of $LiPF_6$ in ethylene carbonate (EC)–dimethyl carbonate (DMC) (1:1, v/v). Microporous polypropylene film (Celgard 2400) was used as the separator. A combination of 85 wt.% $Li_4Ti_5O_{12}$ with 8 wt.% conductive carbon Super P (NCM HERSBIT Chemical Co., LTD., China) and 7 wt.% polyvinylidene fluoride (PVDF) binder homogeneously mixed in N-methyl pyrrolidinone (NMP) were prepared into viscous slurries for efficient deposition. The slurries were deposited on current collectors of copper foil (10 μm) by a blade, which was pretreated by etching with 1 M nitric acid solutions followed by rinsing with water and then acetone. The electrode was then dried under vacuum at 100 °C for 12 h before electrochemical evaluation. Cell assembly was conducted in a glove box filled with pure argon.

2.2. Characterization

The phase structures of the synthesized powders were characterized using an X-ray diffractometer (XRD, ARL X' TRA) with Cu Kα radiation (λ = 0.1541 nm). The experimental diffraction patterns were collected at room temperature by step-scanning in the range of $10° \le 2\theta \le 80°$. The particulate morphology of the $Li_4Ti_5O_{12}$ precursors from the solid-state reaction synthesis and the cellulose-assisted combustion synthesis were examined using an environmental scanning electron microscope (ESEM, QUANTA-2000).

The temperature-programmed oxidation (O_2-TPO) experiment with the solid precursor from the cellulose-assisted combustion synthesis was performed as follows. About 0.1 g of solid precursor was placed into a U-type quartz reactor with an inner diameter of 3 mm. Then, 10 vol.% O_2/Ar (for O_2-TPO) at a flow rate of 20 mL min^{-1} [STP: standard temperature and pressure] was introduced to the reactor. After the gas had been flowing through it at room temperature for 30 min, the reactor was heated to 950 °C at a rate of 10 °C min^{-1}. The effluent gas from the reactor was connected to a Hiden QIC-20 Mass spectrometer (MS) for in situ monitoring of the concentration variations of selected species.

The charge–discharge characteristics of the cells were recorded at different rates over the potential range of 1.0–3.0 V using a NEWARE BTS-5V50 mA computer-controlled battery test station within the temperature range of −20 to 30 °C. Complex impedance measurements of the electrode at 20% depth-of-discharge were carried out at various temperatures using a Princeton Applied Research PARSTAT 2273 advanced electrochemical system over the single cell at of fully charged, fully discharged or discharging states. A perturbation of 10 mV was applied and data were collected under PC control at the applied frequency range of 100 mHz to 1 MHz.

3. Results and discussion

Previously, we have demonstrated that a calcination temperature of 850 °C and a prolonged calcination time of 17 h was necessary to obtain a phase-pure spinel-type $Li_4Ti_5O_{12}$ by the conventional solid-state reaction using TiO_2 anatase and Li_2CO_3 as the reactants. However, by adopting the cellulose-assisted combustion technique with the same TiO_2 anatase as a titanium source, further calcination of the solid precursor at 750 °C for 5 h resulted in the formation of high-purity $Li_4Ti_5O_{12}$ [21]. To obtain information needed to interpret the reduced-temperature synthesis of $Li_4Ti_5O_{12}$ via the cellulose-assisted combustion technique, the solid precursors from both synthesis processes were calcined at various temperatures in air and the resulting powders were subjected to phase-composition analysis.

Fig. 1 shows the XRD patterns of the solid precursor from the cellulose-assisted combustion synthesis and the products obtained by further calcination of the precursor at 400, 500, 600, 700 and 750 °C for 5 h in air. Some Bragg diffraction peaks of weak intensity, assigned to the spinel-type $Li_xTiO_{2+x/2}$ phase, along with the diffraction peaks of the main anatase TiO_2 phase were observed in the XRD patterns of the solid precursor. However, no lithium-related phase was detected, suggesting an amorphous structure of the lithium compounds in the solid precursor. Previously, we have demonstrated that auto-combustion could instantly create a high temperature, which promoted the phase reaction between TiO_2 and the Li-related phase by incorporating Li^+ into the TiO_2 lattice with the formation of a spinel-type $Li_xTiO_{2+x/2}$ composite oxide [21]. The weak diffraction peak intensities suggest the poor crystallinity of the formed $Li_xTiO_{2+x/2}$ phase. The peak intensity of the spinel phase progressively increased relative to the anatase phase with the calcination temperature. At 700 °C, the peak intensity of the anatase phase was substantially reduced as the spinel phase became the dominant phase. The rutile phase, although at weak peak intensity, was also sometimes observed between 400 and 700 °C. After the calcination at 750 °C, only the spinel phase was detected, suggest-

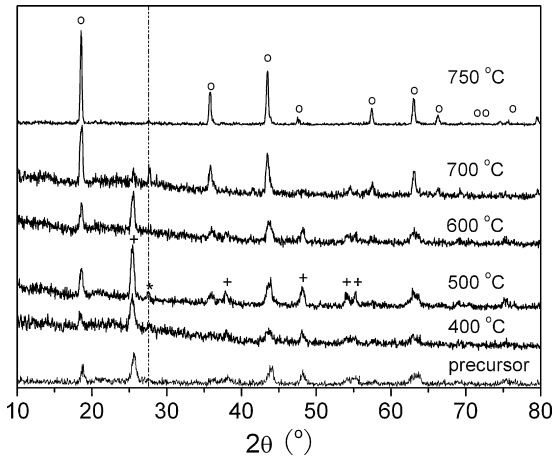

Fig. 1. X-ray diffraction patterns of the solid precursor of $Li_4Ti_5O_{12}$ for the cellulose-assisted combustion synthesis obtained by auto-combustion and the powder products from further calcination of the solid precursor at various temperatures for 5 h in air. (○): spinel $Li_4Ti_5O_{12}$, (*): rutile TiO_2, (+): anatase TiO_2.

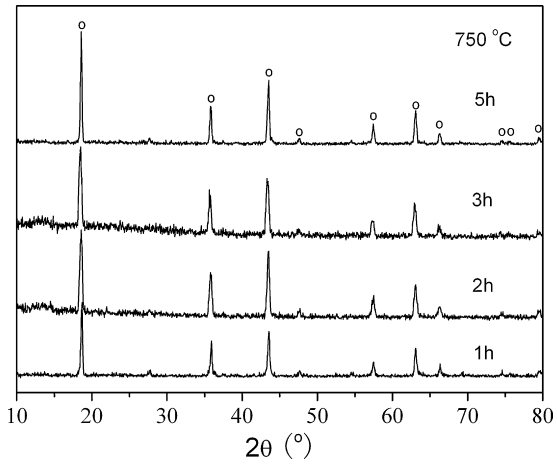

Fig. 2. X-ray diffraction patterns of the samples prepared by the cellulose-assisted combustion process after calcination at 750 °C for different times.

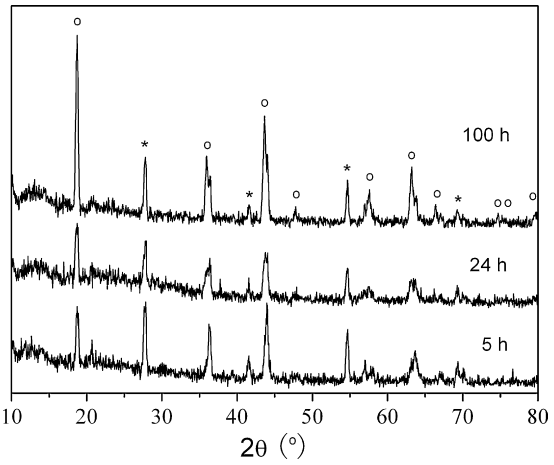

Fig. 4. X-ray diffraction patterns of the samples prepared by solid-state reaction after calcination at 750 °C for various times. (○): spinel $Li_4Ti_5O_{12}$, (*): rutile TiO_2.

ing the successful formation of a phase-pure $Li_4Ti_5O_{12}$ composite oxide. To determine the effect of calcination time on phase formation, the solid precursor was calcined at 750 °C for different periods. As shown in Fig. 2, the oxide displayed the main phase structure of spinel, although a trace amount of TiO_2 rutile was still observed at very weak peak intensity. Such a trace of impurity phase was later found out to have negligible effect on the electrode performance. This suggests the $Li_4Ti_5O_{12}$ composite oxide can be facilely formed by calcination of the solid precursor at 750 °C, agreeing well with our previous observation.

As for the solid-state reaction employing TiO_2 anatase and Li_2CO_3 as the raw materials, large differences in phase-formation behavior were observed. Fig. 3 shows the XRD patterns of the powder products from calcination at various temperatures in air for 5 h of the solid precursor made by the solid-state reaction. The solid precursor showed a physical mixture of TiO_2 anatase and Li_2CO_3, indicating no phase reaction happened during the grinding process. After calcination at 500 °C for 5 h, there was only a minor amount of spinel phase formed, and the sample mainly displayed an anatase phase. At a calcination temperature of 700 °C, the TiO_2 rutile phase appeared with high diffraction peak intensity, while the peak intensity of the TiO_2 anatase phase was reduced substantially. It suggests the TiO_2 anatase was transformed into the rutile phase during the calcination at this temperature. At 850 °C, the rutile phase was still present at notable peak intensity, although the main spinel phase had formed. Phase-pure $Li_4Ti_5O_{12}$ was formed only after calcination at 950 °C for 5 h. To demonstrate whether the failure in the synthesis of phase-pure $Li_4Ti_5O_{12}$ at reduced temperature from the solid-state reaction product was due to insufficient calcination time, the solid precursor was calcined at 750 °C for different times. As shown in Fig. 4, although the relative intensity of the spinel phase with respect to the TiO_2 rutile phase increased with increasing calcination time, a considerable amount of TiO_2 rutile phase was still present even after a calcination time as long as 100 h. This reveals the sluggish nature of the solid-state reaction in the formation of $Li_4Ti_5O_{12}$ and suggests that simply increasing the calcination time is not a practical way to synthesize $Li_4Ti_5O_{12}$.

It is well known that TiO_2 can take several crystalline structures, with the TiO_2 rutile being the most stable one. The TiO_2 anatase is metastable; the thermal treatment could induce the phase transformation of TiO_2 anatase to the more thermodynamically stable TiO_2 rutile phase [22]. To explain the appearance of the TiO_2 rutile phase during the calcination process via the solid-state reaction with TiO_2 anatase as the raw material, the TiO_2 anatase was calcined at various temperatures for 5 h and the oxides obtained were then subjected to phase-composition analysis. Fig. 5 shows the XRD patterns of TiO_2 anatase after calcination at 300–850 °C in air for 5 h. At 700 °C or lower, no obvious phase transition of TiO_2 anatase to TiO_2 rutile was observed. Such a phase transition was still negligible at 750 °C, but greatly promoted at 800 °C. In connection with the results in Fig. 3, the phase-transition temperature of TiO_2 from

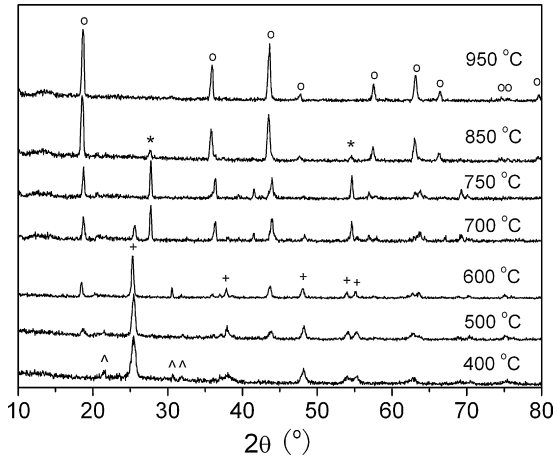

Fig. 3. X-ray diffraction patterns of the samples prepared by solid-state reaction after calcination at various temperatures in air for 5 h. (○): spinel $Li_4Ti_5O_{12}$, (*): rutile TiO_2, (+): anatase TiO_2, (^): Li_2CO_3.

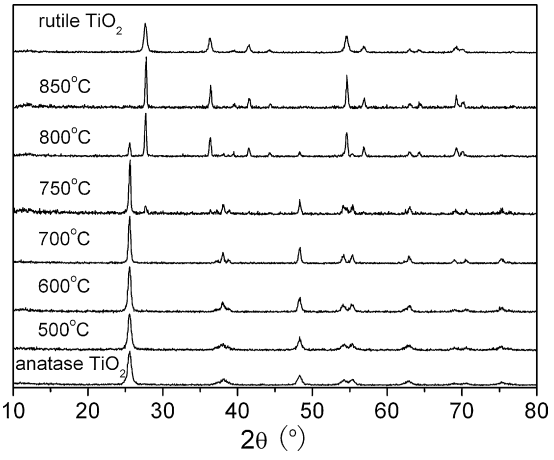

Fig. 5. XRD patterns of TiO_2 after heat treatment at various temperatures in air for 5 h.

anatase to rutile was somewhat lowered for the Li_2CO_3 and TiO_2 mixture. In the prior literature, it has been observed that the phase-transition temperature can be reduced via cation-doping of TiO_2 anatase [23]. Recently, M. Zukalová et al. also mentioned that P-doping would reduce the thermal stability of anatase TiO_2 [24]. These imply that the solid-state reaction between Li_2CO_3 and TiO_2 during the calcination process likely promoted the phase transition of TiO_2 from anatase to rutile.

The solid-phase reaction involves cation and anion diffusion. For the synthesis of $Li_4Ti_5O_{12}$ from TiO_2 and Li_2CO_3, the overall reaction can be expressed as:

$$5TiO_2 + 2Li_2CO_3 \rightarrow Li_4Ti_5O_{12} + 2CO_2\uparrow$$

TiO_2 and Li_2CO_3 have melting points of 1640 °C and 723 °C, respectively. Furthermore, Li^+ has a much higher diffusivity than Ti^{4+}. This suggests that Li_2CO_3 is much more active than TiO_2 at intermediate temperature ranges. As a result, the formation of $Li_4Ti_5O_{12}$ attributed to reactive lithium carbonate reacting with stable titanium dioxide.

During the synthesis, the following reactions could happen competitively:

$$TiO_2\,(\text{anatase}) + Li_2CO_3 \rightarrow Li_4Ti_5O_{12} + CO_2\uparrow \quad (1)$$

$$TiO_2\,(\text{anatase}) \rightarrow TiO_2\,(\text{rutile}) \quad (2)$$

$$TiO_2\,(\text{rutile}) + Li_2CO_3 \rightarrow Li_4Ti_5O_{12} + CO_2\uparrow \quad (3)$$

Since the TiO_2 anatase more easily incorporates lithium than TiO_2 rutile, the transition of TiO_2 from anatase to rutile phase would greatly suppress the formation of $Li_4Ti_5O_{12}$. The appearance of a considerable amount of TiO_2 rutile during the calcination process thus in part explains the high calcination temperature and prolonged calcination time required for the synthesis of $Li_4Ti_5O_{12}$ by the solid-state reaction.

Concerning the much smaller amount of TiO_2 rutile formed during the calcination via the cellulose-assisted combustion synthesis as compared to that in the solid-state reaction process, although a $LiNO_3$ solution was applied as the raw material in the combustion synthesis, the lithium also converted to a solid compound after the auto-combustion. During the auto-combustion process, the high combustion temperature promoted the phase reaction between TiO_2 and lithium with the formation of spinel $Li_xTiO_{2+x/2}$ phase while the phase transition of TiO_2 anatase to TiO_2 rutile was not induced due to the short combustion time. This is an important cause for the reduced synthesis temperature of spinel $Li_4Ti_5O_{12}$ via the combustion technique. During the following calcination process, the reaction between TiO_2 anatase and the lithium compound can also be treated as a solid-phase reaction.

It is well known that solid-state reactions start at the interface of the reactants. The higher the interfacial area of the reactants, the higher reaction rate should be. Fig. 6 shows the SEM images of the precursors of the solid-state reaction and one from the auto-combustion of the cellulose-assisted combustion synthesis. For the precursor from the solid-state reaction, large separated grains were observed, while the raw materials are mixed much more homogeneously and the particles are finer in size in the solid precursor from the cellulose-assisted combustion synthesis, which greatly promoted the phase reaction between TiO_2 and lithium to form the target compound, $Li_4Ti_5O_{12}$.

Previously, we demonstrated that a reducing atmosphere could be created during the auto-combustion process due to the insufficient combustion of the organic during the synthesis [22]. The gray color of the solid precursor suggests there were still considerable organic residuals right after the auto combustion. An O_2-TPO experiment was then conducted on the solid precursor to investigate the oxidation process therein. Fig. 7 shows the gas

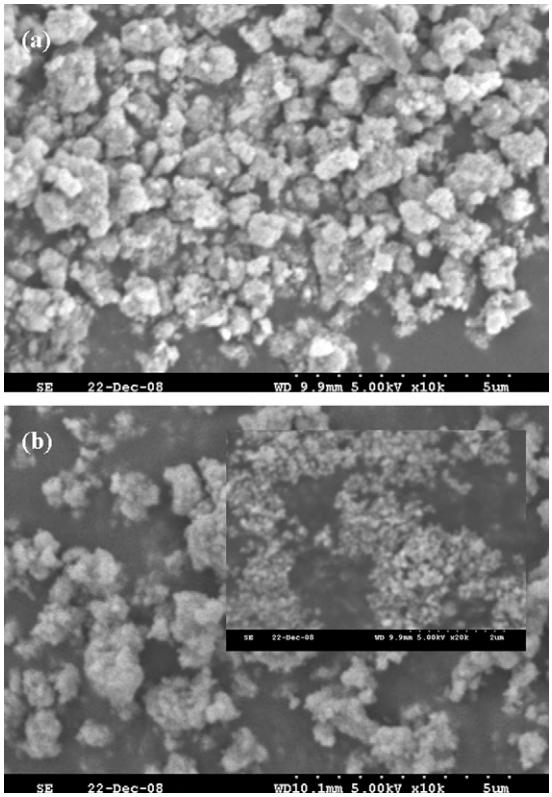

Fig. 6. SEM photos of (a): the precursor from the solid-state reaction of Li_2CO_3 and anatase TiO_2; (b): the solid precursor from the cellulose-GN combustion process.

composition of the effluent gas during the O_2-TPO process. During this process, a considerable amount of the reducing species CO was formed, which created a reducing atmosphere around the reactants. Consequently, the TiO_2 was likely reduced to $TiO_{2-\delta}$ during the high-temperature calcination process. The solid-state reaction between TiO_2 and lithium compound to form $Li_4Ti_5O_{12}$ also involves oxide-ion diffusion. Thereby, the formation of $Li_4Ti_5O_{12}$ via the solid-state reaction is also closely related to the oxygen-ion conductivity of the TiO_2. Indeed, it has been reported that TiO_2 has a certain level of ionic conductivity at elevated temperature [25–27]. Similar to many composite oxides [28,29], oxygen vacancies form the oxygen-ion diffusion path. In a recent literature, Y. Wang et al. reported that by reducing the surface Ti (IV) to Ti (III) of TiO_2, the surface conductivity was improved and the Li-ion diffusion path was shortened during the synthesis process of $Li_4Ti_5O_{12}$ [30]. This implies the reaction rate between TiO_2 and a lithium com-

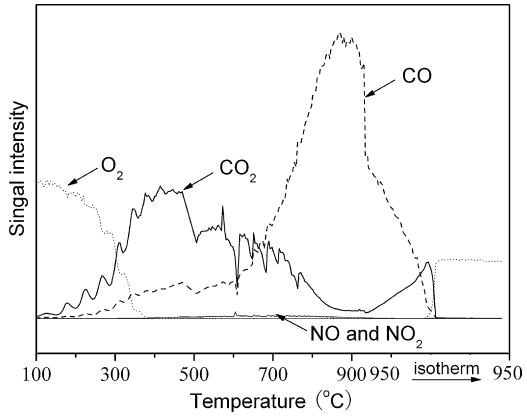

Fig. 7. O_2-TPO profiles of the precursor of cellulose-GN combustion process.

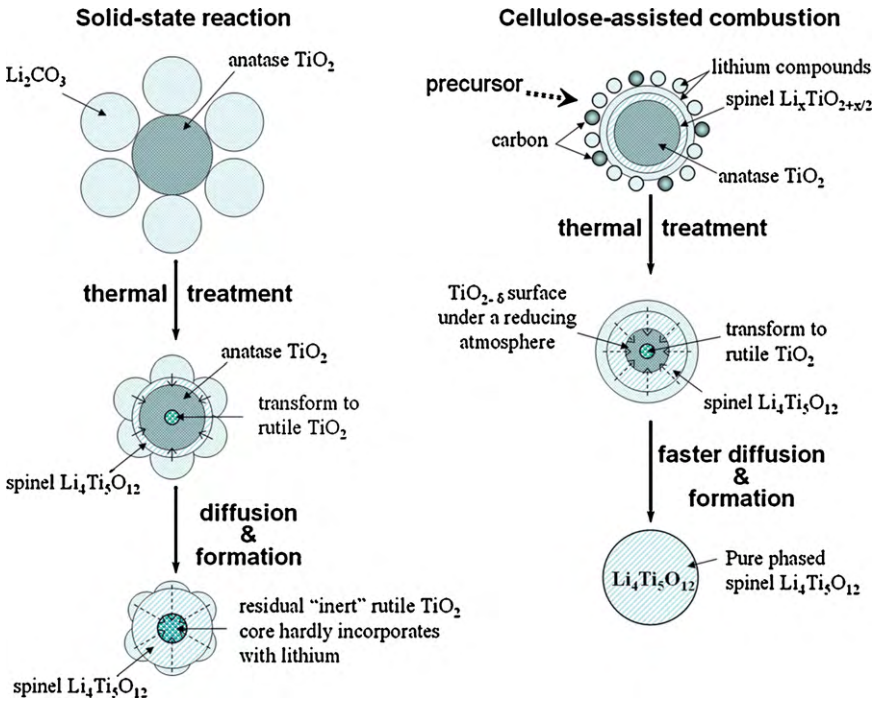

Fig. 8. Mechanism illustration of the solid-state reaction and cellulose-GN processes for $Li_4Ti_5O_{12}$ synthesis.

pound should be promoted under a reducing atmosphere, which promoted the formation of $Li_4Ti_5O_{12}$ spinel phase at a lower temperature.

In view of the reaction mechanisms of the solid-state process and cellulose-assisted combustion process with XRD, SEM and TPO results, mechanism illustrations of reaction process are proposed and illustrated in Fig. 8. Generally, the solid-state reaction between two solid phases is interfacial reaction [31]. As the reaction temperature rises, Li–Ti–O crystal layer formed on the surface of anatase TiO_2 particles. Then Li-ions passing through the layer of Li–Ti–O reacted with anatase TiO_2. At the same time, the phase transition of TiO_2 from anatase to rutile phase occurred. As relatively stable structure, rutile TiO_2 was difficult to react with lithium at a lower calcination temperature. Consequently, very high calcination temperature is needed to facilitate the solid-state reaction between rutile TiO_2 and Li_2CO_3/LiOH to form $Li_4Ti_5O_{12}$ [32,33], which will result in the loss of lithium sources and difficulty in precise control of the cation stoichiometry. For cellulose-GN process, the lithium compounds as an amorphous structure distributed around the anatase TiO_2 homogenously after self-combustion process, resulting in better mixing of both Li and Ti precursors. Spinel-type $Li_xTiO_{2+x/2}$ phase has been partly formed in the precursor, so that the subsequent formation of pure phased spinel-type $Li_4Ti_5O_{12}$ becomes faster. Furthermore, cellulose thermal pyrolysis created a reducing atmosphere, which improved the surface conductivity and shortened the Li-ion diffusion path. Therefore, all the factors mentioned above then accounted for the synthesis of $Li_4Ti_5O_{12}$ at a lower temperature (750 °C) via the cellulose-combustion technique. The promoted formation of $Li_4Ti_5O_{12}$ phase then suppressed the appearance of the TiO_2 rutile phase during the synthesis.

The reduced temperature of the cellulose-assisted combustion synthesis thus resulted in a higher surface area and less aggregation of the $Li_4Ti_5O_{12}$ than that prepared from the traditional solid-state reaction. The smaller grain size suggests a shorter diffusion distance, while a higher surface area means more interfacial reaction sites; both are beneficial for a higher reaction rate performance. Fig. 9 shows the discharge capacity of the $Li_4Ti_5O_{12}$ anodes at various temperatures at a 1 C rate with the powders synthesized by the cellulose-assisted combustion synthesis after calcination at 750 °C for 2 h and from the standard solid-state reaction after calcination at 850 °C for 17 h. The anodes prepared from both synthesis techniques reached the theoretical value of 175 mAh g^{-1} at an operating

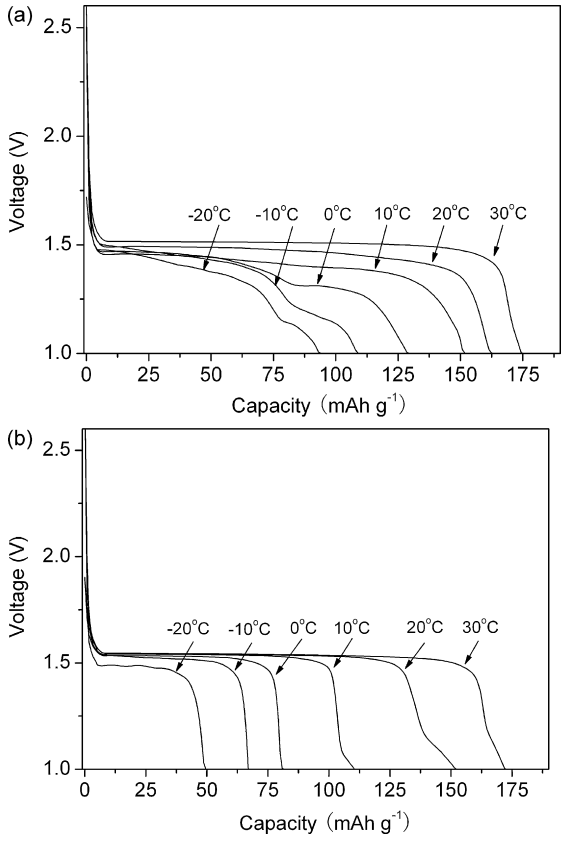

Fig. 9. The discharge profiles of the $Li_4Ti_5O_{12}$ anodes from 1 to 3 V at a 1 C rate at various temperatures; (a) prepared from the cellulose-assisted process and further calcined at 750 °C for 2 h, (b) the solid-state reaction product calcined at 850 °C for 17 h.

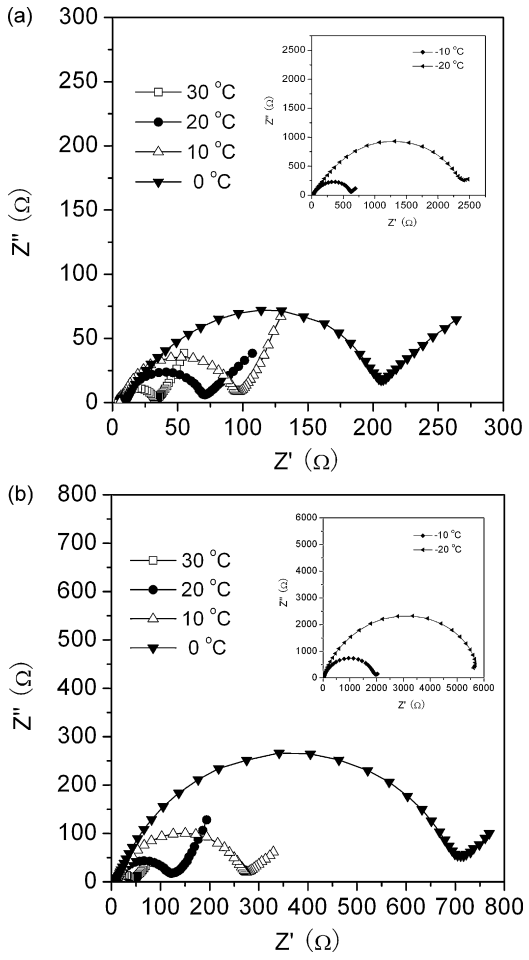

Fig. 10. Complex impedance plots of the half cell with an $Li_4Ti_5O_{12}$ anode prepared by (a) cellulose-assisted combustion synthesis calcined at 750 °C for 2 h; (b) solid-state reaction calcined at 850 °C for 17 h.

temperature of 35 °C with good cycling stability. However, with a decrease in operating temperature, the capacity of the anode prepared from the solid-state reaction decayed quickly, reaching only 49.6 mAh g^{-1} at −20 °C, while the anode prepared from the cellulose-assisted combustion synthesis still retained a capacity of 94.1 mAh g^{-1}. Fig. 10 shows the EIS of both cells at selected temperatures. The electrode-polarization resistance increased sharply for the cell with the $Li_4Ti_5O_{12}$ derived from the standard solid-state reaction, while the increment was much less for the cell with the cellulose-assisted combustion-synthesized $Li_4Ti_5O_{12}$. The larger polarization associated with the $Li_4Ti_5O_{12}$ from the solid-state reaction is due to the larger grain size, resulting from the high calcination temperature necessary for obtaining the phase-pure anode.

4. Conclusions

During the synthesis of $Li_4Ti_5O_{12}$ from TiO_2 anatase, the phase transition of TiO_2 from anatase to the more stable rutile phase and the solid-phase reaction between TiO_2 and the lithium compound happened competitively. TiO_2 rutile has a much lower reactivity with lithium; the formation of TiO_2 rutile then required a higher calcination temperature to obtain phase-pure $Li_4Ti_5O_{12}$. Via the cellulose-assisted combustion synthesis, the near-instant combustion rapidly created a high temperature, which promoted lithium incorporation into the TiO_2 without the anatase-to-rutile phase transition of TiO_2 during the auto-combustion process. It also resulted in a much more homogenous mixing of the raw materials and a much finer particle size of the reactants, which was beneficial for the reaction to proceed at lower temperature. Furthermore, a reducing atmosphere was created during the calcination process of the solid precursor from cellulose-assisted synthesis, due to the insufficient oxidation of the residual organic matter, promoting oxygen-ion diffusion. All the above factors then facilitated the reaction of TiO_2 and the lithium compound to form $Li_4Ti_5O_{12}$. As a result, high-purity $Li_4Ti_5O_{12}$ was formed at 750 °C within a short time (1–5 h) before the phase transition of TiO_2 from anatase to rutile occurred to any significant extent. As for the solid-state reaction, the transition of TiO_2 anatase to rutile occurred during the calcination process, which further increased the difficulty of $Li_4Ti_5O_{12}$ formation. As a result, calcination at ~950 °C for 5 h (or 850 °C for 17 h) is necessary to obtain phase-pure $Li_4Ti_5O_{12}$. Due to the reduced-synthesis temperature, the as-obtained powder from the cellulose-assisted combustion synthesis showed much better low-temperature electrochemical performance. It may find potential practical applications in batteries for electric vehicles working at low-temperature conditions.

Acknowledgments

This work was supported by the “Outstanding Young Scholar Grant at Jiangsu Province” under contract No. 2008023 and the National Basic Research Program of China under contract No. 2007CB209704.

References

[1] A.N. Jansen, A.J. Kahaian, K.D. Kepler, P.A. Nelson, K. Amine, D.W. Dees, D.R. Vissers, M.M. Thackeray, J. Power Sources 81–82 (1999) 902–905.
[2] P.P. Prosini, R. Mancini, L. Petrucci, V. Contini, P. Villano, Solid State Ionics 144 (2001) 185–192.
[3] S Patoux, L. Daniel, C. Bourbon, H. Lignier, C. Pagano, F.L. Cras, S. Jouanneau, S. Martinet, J. Power Sources 189 (2009) 344–352.
[4] E. Matsui, Y. Abe, M. Senna, A. Guerfi, K. Zaghib, J. Am. Ceram. Soc. 91 (5) (2008) 1522–1527.
[5] T. Kostlánová, J. Dědeček, P. Krtil, Electrochim. Acta 52 (2007) 1847–1856.
[6] J. Shu, Electrochim. Acta 54 (2009) 2869–2876.
[7] R.P. Gunawardane, J.G. Fletcher, M.A.K.L. Dissanayake, R.A. Howie, A.R. West, J. Solid State Chem. 112 (1994) 70–72.
[8] J.C. Mikkelsen, J. Am. Ceram. Soc. 63 (1980) 331–335.
[9] G. Izquierdo, A.R. West, Mater. Res. Bull. 15 (1980) 1655–1660.
[10] R. Moshtev, B. Johnson, J. Power Sources 91 (2000) 86–91.
[11] K. Sawai, Y. Iwakoshi, T. Ohzuku, Solid State Ionics 69 (1994) 273–283.
[12] M. Winter, J.O. Besenhard, M.E. Spahr, P. Novák, Adv. Mater. 10 (1998) 725–763.
[13] D. Aurbach, E. Zinigrad, Y. Cohen, H. Teller, Solid State Ionics 148 (2002) 405–416.
[14] T. Ohzuku, A. Ueda, N. Yamamoto, J. Electrochem. Soc. 142 (1995) 1431–1435.
[15] D. Peramunage, K.M. Abraham, J. Electrochem. Soc. 145 (1998) 2609–2615.
[16] G.G. Amatucci, F. Badway, A.D. Pasquier, T. Zheng, J. Electrochem. Soc. 148 (2001) 930–939.
[17] S.H. Huang, Z.Y. Wen, J.C. Zhang, Z.H. Gu, X.H. Xu, Solid State Ionics 177 (2006) 851–855.
[18] L. Kavan, M. Grätzel, Electrochem. Solid-State Lett. 5 (2002) A39–A42.
[19] E. Ferg, R.J. Gummov, A.de. Kock, M.M. Thackeray, J. Electrochem. Soc. 141 (1994) L147–L150.
[20] X.L. Yao, S. Xie, C.H. Chen, Q.S. Wang, J.H. Sun, Y.L. Li, S.X. Lu, Electrochim. Acta 50 (2005) 4076–4081.
[21] T. Yuan, K. Wang, R. Cai, R. Ran, Z.P. Shao, J. Alloys Compd. 477 (2009) 665–672.
[22] C. Perego, R. Revel, O. Durupthy, S. Cassaignon, J.P. Jolivet, Solid State Sci. 12 (2010) 989–995.
[23] C.K. Lee, C.C. Wang, M.D. Lyu, L.C. Juang, S.S. Liu, S.H. Hung, J. Colloid Interface Sci. 316 (2007) 562–569.
[24] M. Zukalová, J. Procházka, A. Zukal, J.H. Yum, L. Kavan, M. Graetzel, J. Electrochem. Soc. 157 (2010) H99–H103.
[25] J. Nowotny, M. Radecka, M. Rekas, S. Sugihara, E.R. Vance, W. Weppner, Ceram. Int. 24 (1998) 571–577.
[26] J.F. Baumard, E. Tani, Phys. Stat. Sol. A 39 (1977) 373–382.
[27] D.C. Cronemeyer, Phys. Rev. 87 (1952) 876–886.

[28] L. Ge, W. Zhou, R. Ran, S.M. Liu, Z.P. Shao, W.Q. Jin, N.P. Xu, J. Membr. Sci. 306 (2007) 318–328.
[29] P.Y. Zeng, Z.P. Shao, S.M. Liu, Z.P. Xu, Purif. Technol. 67 (2009) 304–311.
[30] Y. Wang, H. Liu, K. Wang, H. Eiji, Y. Wang, H. Zhou, J. Mater. Chem. 19 (2009) 6789–6795.
[31] A. Beauger, J.C. Mutin, J.C. Niepce, J. Mater. Sci. 18 (1983) 3543–3550.
[32] S.H. Huang, Z.Y. Wen, X.J. Zhu, Z.H. Gu, Electrochem. Commun. 6 (2004) 1093–1097.
[33] S.H. Huang, Z.Y. Wen, X.J. Zhu, Z.X. Lin, J. Electrochem. Soc. 152 (1) (2005) A186–A190.